PHYSICAL REVIEW E **67**, 065603(R) (2003)

Influence of spatial correlations on the lasing threshold of random lasers

Michael Patra
Laboratory for Computational Engineering, Helsinki University of Technology, P. O. Box 9203, 02015 HUT, Finland
(Received 18 February 2003; published 27 June 2003)

The lasing threshold of a random laser is computed numerically from a generic model. It is shown that spatial correlations of the disorder in the medium (i.e., dielectric constant) lead to an increase of the decay rates of the eigenmodes and of the lasing threshold. This is in conflict with predictions that such correlations should lower the threshold. While all results are derived for photonic systems, the computed decay rate distributions also apply to electronic systems.

DOI: 10.1103/PhysRevE.67.065603 PACS number(s): 42.25.Dd, 42.55.Zz, 05.40.−a, 72.15.Rn

In the theory of disordered media, two important regimes, diffusive and localized, are distinguished [1]. In the diffusive regime (for a weak or moderate disorder), eigenstates are extended and efficient transport is possible. In the localized regime (for a strong disorder), eigenstates become localized and transport is strongly inhibited. Many experimental findings for random lasers are more consistent with the assumption of a lasing mode that is localized, while a direct experimental analysis of the sample shows that it is in the diffusive regime.

To determine whether a sample is in the localized or in the diffusive regime, a transport property is measured. The most efficient way to achieve this is to check for the rounding of the backscattering cone [2]. Such a rounding is not reported from experiments [3,4]. Transport is, however, dominated by extend eigenstates, and the simultaneous existence of a few localized eigenstates in a sample in the diffusive regime, i.e., *on an average*, diffusive, would not be noticed [5]. Such localized modes have recently been detected experimentally in a diffusive sample [6].

The important question is to explain under which conditions such localized eigenstates can exist in a diffusive sample. (These states have been termed anomalously localized states or prelocalized states. For a recent review, see Ref. [7].) One-dimensional disordered systems are always in the localized regime, i.e., these systems can never show diffusive behavior. Theoretical studies on such systems thus cannot give information on the interplay between extended and localized modes. The situation is different in two- and three-dimensional samples. Two-dimensional samples shorter than the localization length behave similar to three-dimensional samples, and one is allowed to replace three-dimensional systems with their computationally cheaper two-dimensional counterparts.

The computational cost of treating a two-dimensional sample is significantly higher than for a one-dimensional sample, and only few studies have been published [8]. Reference [5] models the scatterers in the disordered media as dipoles, Ref. [9] studies circular particles using the finite-difference time-domain (FDTD) method. Both publications do not state explicitly whether their samples are in the diffusive or in the localized regime, but the parameters given strongly suggest that the samples are in the localized regime.

The only publication so far on the interplay between the diffusive and the localized eigenstates inside a diffusive sample seems to be Ref. [10]. There, it was estimated that localized states become exponentially more frequent when the disorder inside the sample is spatially correlated. Motivated by the picture of photons traveling in a closed loop inside a ring-shaped structure [3], they study a ring-shaped area of higher dielectric constant. This is a very special situation, and it is not obvious how characteristic such a special situation is for the entire behavior. (It should be noted that the opposite effect, namely, in a localized sample a few modes become extended when spatial correlations in the disorder are introduced, is well understood, see, e.g., Ref. [11].)

In this paper, we will study this problem from a more generic approach. The lasing threshold of a sample is determined by the decay rates of the eigenstates of the system since the loss (=decay) of photons in the mode has to be compensated by pumping if the sample is to start the lasing action. Following the approach of Ref. [12] we numerically compute the decay rate distribution of a two-dimensional sample on a suitable grid. (Earlier work on the lasing threshold of chaotic cavities [13] cannot be applied since by construction all eigenstates are extended [1].) We improve on previous work by including spatial correlations.

We use the Anderson Hamiltonian which describes the motion of an uncharged particle in a spatially varying potential. The Schrödinger equation for electronic systems with spatially varying potential has (at constant energy) the same form as the Helmholtz equation for photonic systems with a spatially varying dielectric constant. Our results can thus directly be applied also to photonic systems. The sample is discretized with lattice spacing Δ, where for electronic systems $\Delta=\pi/k_F$ (k_F is the wave vector at the Fermi level) and for photonic systems $\Delta=2\lambda/\pi$ (λ is the wave length of the light). This is a natural choice in which there is then precisely one propagating mode per transversal lattice point, and the width of the sample is best measured in terms of the number N of propagating modes.

Transport is modeled by nearest-neighbor hopping with rate 1. (The results are easily adapted to an arbitrary speed c of transport.) With a spatially varying potential $P(x,y)$, the Hamiltonian for a sample of length $L=\tilde{L}\Delta$ becomes [12]

$$\mathcal{H}_{(x,y),(x',y')}=\delta_{xx'}\delta_{yy'}[P(x,y)-i(\delta_{1y}+\delta_{Ly})]+\delta_{yy'}(\delta_{x+1,x'}+\delta_{x-1,x'})+\delta_{x,x'}(\delta_{y+1,y'}+\delta_{y-1,y'}), \quad (1)$$

with $x=1,\ldots,\tilde{L}$ and $y=1,\ldots,N$. The imaginary part of $\mathcal{H}$ models coupling of the sample to the outside where we assume that we operate at the center of the conduction band.

The spatial correlations are assumed to fall of exponentially such that $P(x,y)$ takes on random values, normal distributed with zero mean and correlator

$$\langle P(\vec{r})P(\vec{r}')\rangle = w^2 \exp\left(-\frac{|\vec{r}-\vec{r}'|}{R_c}\right). \tag{2}$$

Here, w measures the strength of the disorder and R_c is the correlation radius. Since we need to generate a large number of mutually correlated random numbers, a Fourier based method has to be employed [14].

The eigenvalues of the matrix $\mathcal{H}$ correspond to the eigenmodes of the system. Their real part ω gives the energy (or, for photonic systems, the frequency) of the mode, and their imaginary part γ the decay rate [15]. We thus have an eigenvalue problem of a non-Hermitian complex symmetric matrix, but an eigensolver specifically adopted to this structure exists [12]. Even with this efficient eigensolver, this is still a numerically expensive task, and it is impossible to analyze so many samples that there would be no more noise in the results.

While the model is described in terms of the disorder strength w, contact with experiments or analytical theories is best made by introduction of the mean-free path l. It can be computed from the length dependence of the transmission probability T through the sample. In the diffusive regime, $l \lesssim L \ll Nl$, it is given by [1]

$$\frac{1}{T} = 1 + \frac{L}{l}. \tag{3}$$

The transmission probability has been computed using the method of recursive Green's functions [16] for a variable disorder strength w and correlation length R_c. We determined the mean-free path by fitting the numerically computed $T(L)$ to this functional form self-consistently in the interval $[l;10\,l]$. (Picking some other interval, e.g., $[0;l]$, changed the result only by about 1%.) The rescaled results are depicted in Fig. 1 for both $N=51$ and $N=81$, i.e., for samples of different width. As figure shows, both sets of curves are almost identical, thereby demonstrating that we are operating in the wide-sample regime. The mean-free path increases significantly as R_c increases. This is immediately obvious since with increasing R_c the potential changes less within a given distance; hence, there is less scattering.

We would like to point out two ''curiosities.'' The numerical data suggest that the mean-free path l factorizes as $l(w,R_c)=f_1(w)f_2(R_c)$. We did not manage to find an explanation for this observation. Furthermore, the mean-free path seems to scale as $l \propto w^{-1.71}$, where 1.71 is a numerical parameter. For an uncorrelated random order that is uniformly distributed in the interval $[-w;w]$, a scaling $l \propto w^{-1.5}$ was found numerically [12]. An analytical theory is available only for one-dimensional systems in the limit $w \to 0$ where $l \propto 1/w^2$ is found [17], so that a universal scaling for a finite w might not exist at all.

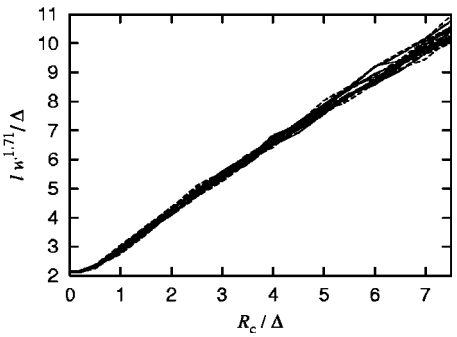

FIG. 1. Numerically computed rescaled mean-free path l, depending on the disorder strength w and the correlation radius R_c (in units of the lattice spacing Δ). The solid lines are for samples of width $N=51$, the dashed lines for samples of width $N=81$. Samples were computed with w in steps of 0.1 and R_c in steps of 0.5Δ (plus the value $R_c=0.2\Delta$). By rescaling $l \to l w^{1.71}$, we can demonstrate the apparent scaling $l \propto w^{-1.71}$ and the factorization $l(w,R_c)=f_1(w)f_2(R_c)$.

The increase of l with increasing R_c poses a problem for a systematic study of the effects of correlations. One has to decide whether to compare samples with identical l (and thus variable w) or samples with identical w (and thus variable l). The final results must depend (apart from trivial prefactors) only on the ratios L/l and R_c/l—not on any of those quantities separately. This decision is thus ''only'' one of numerical efficiency and minimization of finite-size effects.

For most of our simulations, we have decided to keep l constant at $l=12.5\Delta$. For each value of R_c, the needed value for w was determined by interpolation of the numerical data presented in Fig. 1. The choice of constant l offers the advantage that, even if R_c is changed, samples with identical ''physical'' length L/l occupy the same number of lattice points, and thus need the same amount of numerical work. [For constant physical length L/l, the needed computing time scales as $O(l^2)$. With constant w, this would impose severe restrictions on the range of R_c that could be treated.]

We have computed the decay rates for samples of width $N=50$ for length $L/l=1,2,3,4,5,6,9,12,15,18$, and correlation radius $R_c/\Delta=0.0,0.2,0.5,1.0,1.5,\ldots,7.5$. For each set of parameters, approximately 2000 samples were generated. The maximum value of L is limited because we are interested in the diffusive regime, hence L has to be sufficiently smaller than the localization length $L_{loc}=(N+1)l/2$. We did not consider larger values of R_c than 7.5Δ since the sample should be much wider than the characteristic length scale of the disorder. Otherwise, the sample would effectively become one dimensional.

To check the results, we have computed the decay rate distribution also for $N=80$ for a few selected values of L/l and R_c. To complement the other simulations, we have kept w constant. As explained above, this implies that we could only include $R_c \leqslant 2\Delta$.

Following the approach introduced in Ref. [12] for samples in the diffusive regime, we fit the numerically computed decay rate distribution to the functional form

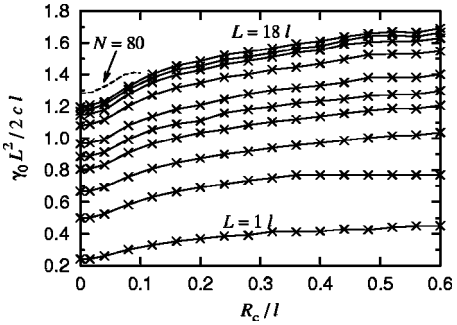

FIG. 2. Characteristic decay rate γ_0 as a function of sample length L and correlation radius R_c (for samples of width $N=50$). The dashed line is for the control simulations with $N=80$ and $L=25l$.

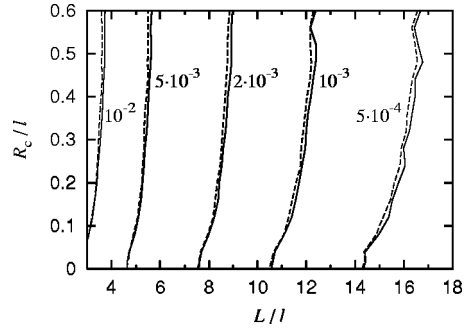

FIG. 3. Comparison of the average of the lasing threshold, directly computed from the numerical data (solid line), and the most likely lasing threshold computed from the distribution of the individual decay rates (dashed line). Both lines have been computed from the same samples, explaining the correlation of the noise in the two sets of lines.

$$\mathcal{P}(\gamma)=\frac{\gamma_0^2}{\gamma^2}\left[1-Q\left(M+1,\frac{M\gamma}{\gamma_0}\right)\right], \tag{4}$$

where the fitting parameters M and γ_0 depend on N, L, and R_c, and $Q(a,x)\equiv\Gamma(a,x)/\Gamma(a)$ is the regularized Gamma function .

All numerically computed histograms fit well to the form (4). The dependence of $P(\gamma)$ onto M is only weak for $M\gg1$, making a precise determination of M difficult. Within this error limit, we did not find a significant dependence of M on R_c, and M is approximately given by the $R_c=0$ result, $M=N/[1+L/(6l)]$ [12].

The fitting parameter γ_0, marking the typical value of the decay rates, can be determined to much better precision. γ_0 is much more important for the lasing threshold than M, so the limited precision of M does not pose a problem. The determined γ_0 is shown in Fig. 2.

For $R_c=0$, $\gamma_0 L^2$ seems to approach a constant value as L is increased. This value is about 20% larger than the value $1/(2cl)$ found numerically for equidistributed disorder in the interval $[-w;w]$ [12]. Trying to approach the limit $L\to\infty$ numerically is not possible since then the sample would become localized.

The important conclusion from Fig. 2 is that for samples of arbitrary lengths, the introduction of correlations in the disorder leads to an increase of the decay rates. This increase is quick as R_c is increased starting from 0, and becomes slower for large R_c. The same behavior is seen in the control simulations with $N=80$ and a fixed w (and thus variable l).

Until now, all results are valid for both electronic and photonic systems. Now we will specialize to random lasers. The light inside a random laser is amplified by a laser dye. This dye is able to amplify light within a certain range of frequencies, so only $K\gg1$ eigenmodes out of all eigenmodes of the system are amplified. This number varies only slightly between different realizations of the same ensemble due to an effect known as spectral rigidity [1]. The lasing threshold is given by the smallest decay rate out of the K modes within the amplification window [18]. This is immediately obvious since the lasing threshold is passed when photons are created faster than they can decay (=escape from the sample).

There are two different approaches to compute the lasing threshold of a random laser. The direct approach is to compute the eigenmodes of a certain number of realizations of the disordered systems, then for each realization to determine the smallest decay rate inside the amplification window, and finally collect statistics for those values. Since this process yields only a single datum per sample, a very large number of realizations needs to be computed to arrive at data of sufficient quality. The average lasing threshold determined in this way is depicted in Fig. 3 as dashed line.

Frequently more efficient is the second approach where one starts with the computation of the distribution $P(\gamma)$ of the individual decay rates. The intermediary result is either a numerical histogram, or, by fitting the histogram to an analytical form, a distribution function that can be evaluated directly for an arbitrary argument. We adopt the latter and use Eq. (4) together with the values of M and γ_0 computed by fitting.

The distribution $P_l(\gamma_l)$ of the lasing threshold is the distribution of the smallest value out of the K values, each distributed according to $P(\gamma)$. This assumes that the decay rates of different modes are uncorrelated. For $K\gg1$ this seems logical, but to the best of our knowledge no explicit check of this assumption has been published so far. As a side effect of our computations, we will fill this gap.

$P_l(\gamma_l)$ is difficult to evaluate numerically for $K\gg1$ since it is sharply peaked. The position γ_m of the maximum of P_l is immediately seen to be given by

$$0=\frac{dP(\gamma_m)}{d\gamma_m}\left[1-\int_0^{\gamma_m}P(\gamma')d\gamma'\right]-(K-1)[P(\gamma_m)]^2. \tag{5}$$

Since P_l is that sharply peaked, γ_m already contains all the relevant information, and nothing relevant is lost by not computing the entire distribution. The lasing threshold computed from Eq. (5), after inserting the fitting parameters M and γ_0 computed from the numerical histograms into Eq. (4), is shown as solid line in Fig. 3.

From the figure, two important conclusions can be drawn. First, the lasing threshold computed via the two separate

methods agrees well. (The noise of the two sets of curves is correlated since the same raw data were used as input for both methods.) This means that the decay rates of different modes indeed are uncorrelated. Furthermore, also fitting the numerical histogram to the form (4) is a valid procedure.

The second conclusion—the heart of this paper—is that introducing spatial correlations into the disorder of a random laser increases the lasing threshold, in contradiction to predictions [10].

In this paper, we have thus arrived at two related—but not identical—results. We have shown that the characteristic decay rates increase if spatial correlations of the disorder are introduced (cf. Fig. 2). The computed decay rate distribution possesses the same form, just with different parameter, as earlier observed for diffusive samples with uncorrelated disorder [12]. This first result means that the ''typical'' eigenstates become more lossy.

Our second result is that the lasing threshold also increases (cf. Fig. 3). This means that also the ''special'' eigenstates with lower-than-average loss, which are selected by mode competition to become the lasing modes, become more lossy. Even though we did not directly compute the spatial extend of the eigenstates, this still clearly demonstrates that no localized (or prelocalized) eigenstates are formed by the introduction of spatial disorder. We thus fail to observe the prediction that such states should be created [10].

There are several explanations for the difference between our results and Ref. [10]. One explanation is that a single ring-shaped area of increased dielectric constant does lead to the formation of a localized state, as suggested by the authors, but the influence of the disorder around that ring-shaped area significantly reduces this effect. Another, equally likely, explanation is that in our simulations, we are only able to treat samples of finite size, with a finite number of eigenstates. The creation of a localized state may be an event that is so rare the we fail to see such an event occur in our finite-size simulations. On the other hand, the typical length scale is given by the area per lasing mode, measured experimentally to be a few 10 μm^2 in two-dimensional ZnO films [19], and our samples are larger than this.

To give a definite answer on whether spatial correlations can explain the formation of localized states, more numerical studies are needed, preferably using different methods. Specialized but numerically efficient models [5] cannot incorporate spatial correlations of the dielectric constant. Two-dimensional FDTD simulations have already been used to describe random lasers [9]. These need to make only minimal assumptions and can be extended to include arbitrary spatial correlations. FDTD simulations thus might be a good candidate, but diffusive samples need to be larger than the localized samples studied so far. Given that FDTD is computationally very expensive, it is not obvious to us whether this would still be numerically feasible.

This work was supported by the European Union Marie Curie program under Grant No. HPMF-CT-2002-01794.

[1] C.W.J. Beenakker, Rev. Mod. Phys. **69**, 731 (1997).
[2] F.J.P. Schuurmans, M. Megens, D. Vanmaekelbergh, and A. Lagendijk, Phys. Rev. Lett. **83**, 2183 (1999).
[3] H. Cao *et al.*, Phys. Rev. Lett. **82**, 2278 (1999); Phys. Rev. B **59**, 15 107 (1999); Phys. Rev. E **61**, 1985 (2000).
[4] G. van Soest, F.J. Poelwijk, R. Sprik, and A. Lagendijk, Phys. Rev. Lett. **86**, 1522 (2001).
[5] A.L. Burin, M.A. Ratner, H. Cao, and R.P.H. Chang, Phys. Rev. Lett. **87**, 215503 (2001).
[6] H. Cao, Y. Ling, J.Y. Xu, and A.L. Burin, Phys. Rev. E **66**, 025601 (2002).
[7] A.D. Mirlin, Phys. Rep. **326**, 259 (2000).
[8] There has been a large number of studies using the diffusion approximation. Using this approximation is numerically very efficient but forbids the existence of localized states. These studies thus cannot explain the interplay between extended and localized eigenstates.
[9] P. Sebbah and C. Vanneste, Phys. Rev. B **66**, 144202 (2002).
[10] V.M. Apalkov, M.E. Raikh, and B. Shapiro, Phys. Rev. Lett. **89**, 016802 (2002).
[11] F.M. Izrailev and A.A. Krokhin, Phys. Rev. Lett. **82**, 4062 (1999).
[12] M. Patra, Phys. Rev. E **67**, 016603 (2003).
[13] M. Patra, H. Schomerus, and C.W.J. Beenakker, Phys. Rev. A **61**, 23810 (2000); K.M. Frahm *et al.*, Europhys. Lett. **49**, 48 (2000); H. Schomerus *et al.*, Physica A **278**, 469 (2000).
[14] B. Kozintsev, Ph.D. thesis, University of Maryland, College Park, 1999.
[15] Actually, the imaginary part of the eigenvalue differs by a factor 2 from the definition of the decay rate. The same factor 2 appears in the definition of the lasing threshold such that those two factors cancel. For ease of writing, we will in the following refer to γ as decay rate, not each time mentioning the factor 2.
[16] H.U. Baranger, D.P. DiVincenzo, R.A. Jalabert, and A.D. Stone, Phys. Rev. B **44**, 10 637 (1991).
[17] B. Kramer and A. MacKinnon, Rep. Prog. Phys. **56**, 1469 (1993).
[18] T.S. Misirpashaev and C.W.J. Beenakker, Phys. Rev. A **57**, 2041 (1998).
[19] Y. Ling, H. Cao, A.L. Burin, M.A. Ratner, X. Liu, and R.P.H. Chang, Phys. Rev. A **64**, 063808 (2001).